

REFRACTIVE INDEX AND TEMPERATURE SENSOR BASED ON
LARGE OFFSET DISTANCE OF CORELESS SILICA INTERFEROMETER

NUR FAIZZAH BINTI BAHARIN

A thesis submitted in fulfilment of the
requirements for the award of the degree of
Master of Philosophy

Faculty of Electrical Engineering
Universiti Teknologi Malaysia

JULY 2018

DEDICATION

Specially dedicated to my parents; Baharin and Saripah,
beloved husband, family and friends for their continuous support, prayers and
understanding.

~ With love and respect ~

ACKNOWLEDGEMENT

Bismillahirrahmanirrahim.

Alhamdulillah, all praise to Allah S.W.T. for his guidance, grace and blessing that makes me able to complete my research work. I would like to express my deepest gratitude to my supervisors, Dr. Asrul Izam bin Azmi, Dr. Ahmad Sharmi bin Abdullah and Dr. Muhammad Yusof bin Mohd Noor for their moral support, guidance and inspiration along this journey. I am very indebted for their effort in teaching and guiding me especially in conducting the experimental work and completing the thesis. Without them, I am not able to complete this research work.

It is my privilege to thank my parents, siblings and friends including Fadhilah, Asmanissa, and etc. for their love, prayers and endless moral support especially during the critical period of this research. Not forgotten to my small research group; Musliha Aisha and Normala, thank you for your kindness and priceless help. My appreciations are extended to the members of Photonics Research Group, Encik Ahmad and Puan Ayu for creating an enjoyable working environment and for their technical assistances. The financial support from MyBrain15 and UTM research grant are also kindly appreciated. Finally, thank you to those who helped me directly or indirectly in completing my study.

ABSTRACT

This thesis reports an original research on the development of refractive index (RI) sensor based on all-fiber Mach Zehnder Interferometer (MZI). The research development process involved design and analysis of sensor structure using BeamPROP software, in-house fabrication using pre-determined optical fiber splicing recipe and experimental work for verifying sensing performance. The fiber MZI sensor was realized from symmetrical offset of coreless silica fiber (CSF), where a section of CSF was spliced between two CSF sections in an offset manner. Thus, two distinct optical paths were created with large index difference, the first path through the connecting CSF sections and the second path at the outside of CSF through the surrounding media. RI sensing was established from direct interaction of light with surrounding media, hence high sensitivity can be achieved with a relatively compact sensor size. The use of CSF purposely to reduce the complexity of sensor fabrication as large diameter of CSF allows lower tolerance of getting the optimum offset distance. The offset distance was optimized using BeamPROP software for maximum fringe visibility at different sensor lengths. Fabrication recipe was meticulously refined and successfully employed in manufacturing the lateral offset structure. Three samples of sensor with different MZI arm length of 0.5 mm, 1.0 mm and 1.5 mm were experimented for (RI) sensing. The highest sensitivity of 1025 nm/RIU was recorded by the sensor of 1.0 mm arm length for RI range between 1.335 and 1.350. The flexibility of the sensor structure was further manifested in temperature sensing by filling the secondary path with high-thermo-optic material. Substantial temperature sensitivity enhancement from 28 pm/°C to 3220 pm/°C was achieved with regard to the original air filled secondary path structure. With the main attributes of high RI/temperature sensitivity and compact size, the proposed sensor would be an attractive sensing tool for many applications including include blood diagnosis, water quality control and food industries in near future.

ABSTRAK

Tesis ini melaporkan penyelidikan asal perkembangan sensor indeks bias (RI) berdasarkan semua-gentian *Mach Zehnder Interferometer* (MZI). Proses pembangunan penyelidikan ini melibatkan reka bentuk dan analisis struktur sensor menggunakan perisian BeamPROP, fabrikasi dalaman dengan menggunakan resipi sambungan gentian optik yang telah ditentukan dan kerja eksperimen untuk mengesahkan prestasi penderiaan. Sensor gentian MZI telah direalisasikan dari ofset simetri gentian silika tidak berteras (CFS), di mana satu bahagian CSF telah disambung di antara dua bahagian CSF dengan caraimbangan. Oleh itu, dua laluan optik yang berbeza telah dihasilkan dengan perbezaan indeks yang besar, laluan pertama adalah melalui bahagian cantuman CSF dan laluan kedua adalah di luar CSF melalui media sekitar. Penginderaan RI ditubuhkan dari interaksi langsung cahaya dengan media sekitar, maka kepekaan yang tinggi dapat dicapai dengan saiz sensor relatif yang padat. CSF telah digunakan untuk mengurangkan kerumitan fabrikasi sensor kerana diameter besar CSF membolehkan toleransi yang lebih rendah untuk memperoleh jarak optimum. Jarak ofset dioptimumkan menggunakan perisian BeamPROP untuk penglihatan pinggir maksimum untuk panjang sensor yang berbeza. Resepi fabrikasi telah ditapis dengan teliti dan berjaya digunakan dalam pembuatan struktur mengimbangi sisi. Tiga sampel sensor dengan panjang lengan MZI yang berlainan iaitu 0.5 mm, 1.0 mm dan 1.5 mm telah diuji untuk penderiaan RI. Kepekaan tertinggi 1025 nm/RIU dicatatkan oleh sensor panjang lengan 1.0 mm untuk rentang RI diantara 1.335 dan 1.350. Fleksibiliti struktur sensor dalam penginderaan suhu dengan lebih terperinci diuji dengan mengisi laluan kedua dengan bahan termo-optik tinggi. Peningkatan kepekaan suhu yang besar dari 28 pm/°C hingga 3220 pm/°C telah dicapai berbanding struktur laluan kedua yang diisi udara asli. Dengan ciri-ciri utama kepekaan RI/suhu tinggi dan saiz yang kecil, sensor yang dicadangkan akan menjadi alat pengesanan yang menarik dalam waktu terdekat bagi banyak aplikasi termasuk diagnosis darah, kawalan kualiti air dan industri makanan.

TABLE OF CONTENTS

| CHAPTER | TITLE | PAGE |
|----------------|------------------------------|-------------|
| | DECLARATION | ii |
| | DEDICATION | iii |
| | ACKNOWLEDGEMENT | iv |
| | ABSTRACT | v |
| | ABSTRAK | vi |
| | TABLE OF CONTENTS | vii |
| | LIST OF TABLES | x |
| | LIST OF FIGURES | xi |
| | LIST OF ABBREVIATIONS | xv |
| | LIST OF APPENDICES | xvi |
| 1 | INTRODUCTION | |
| | 1.1 Introduction | 1 |
| | 1.2 Fiber Optic Sensor | 2 |
| | 1.3 Problem Statement | 5 |
| | 1.4 Objectives of Research | 6 |
| | 1.5 Scope of Study | 6 |
| | 1.5.1 Design and simulation | 6 |
| | 1.5.2 Experimental works | 7 |
| | 1.6 Significance of Study | 7 |

| | | |
|----------|--|----|
| 1.7 | Thesis Overview | 8 |
| 2 | LITERATURE REVIEW | |
| 2.1 | Introduction | 10 |
| 2.2 | Types of Fiber Interferometers | 10 |
| 2.2.1 | Fabry Perot Interferometer | 11 |
| 2.2.2 | Michelson Interferometer | 12 |
| 2.2.3 | Mach-Zehnder Interferometer | 13 |
| 2.3 | Methods of implementation MZI | 17 |
| 2.3.1 | Fiber Taper | 17 |
| 2.3.2 | Collapse Region of PCF | 20 |
| 2.3.3 | Peanut Shape Structure | 22 |
| 2.3.4 | Fiber Core Mismatched | 23 |
| 2.4.5 | MZI based on lateral offset structure | 26 |
| 2.4 | Coreless Silica Fiber based RI sensor | 34 |
| 2.5 | Summary | 35 |
| 3 | RESEARCH METHODOLOGY | |
| 3.1 | Introduction | 37 |
| 3.2 | Design Specification and Working Principle | 39 |
| 3.3 | Feasibility Test | 42 |
| 3.4 | Simulation using BeamPROP software | 43 |
| 3.5 | Fabrication Process | 47 |
| 3.6 | Experimental Work and Data Analysis | 50 |
| 3.7 | Summary | 53 |
| 4 | RESULTS AND DISCUSSION | |
| 4.1 | Introduction | 54 |
| 4.2 | BeamPROP Simulation | 55 |
| 4.2.1 | Optimization of Offset Distance | 55 |

| | | |
|----------|--|--------------|
| 4.2.2 | Field Distribution of Sensor Structure | 59 |
| 4.3 | Experimental Result | 61 |
| 4.3.1 | Response of Sensor to Different RI Solutions | 62 |
| 4.3.2 | Response of Sensor to Temperature Changes | 67 |
| 4.3.3 | Long-Term Stability Test | 71 |
| 4.3.4 | Application of the Proposed Structure for Temperature Sensing | 73 |
| 4.4 | Comparison of Interference Spectra Obtained From Simulation and Experimental Work | 77 |
| 4.5 | Summary | 79 |
| 5 | CONCLUSION AND RECOMMENDATION | |
| 5.1 | Introduction | 80 |
| 5.2 | Conclusions | 80 |
| 5.3 | Recommendation for Future work | 83 |
| | REFERENCES | 84-91 |
| | Appendices A - B | 92-94 |

LIST OF TABLES

| TABLE NO. | TITLE | PAGE |
|------------------|---|-------------|
| 2.1 | Comparison between different types of techniques to realized MZI | 30 |
| 3.1 | Parameter used in Table Editor | 45 |
| 4.1 | Optimum offset distance for each sensor sample | 57 |
| 4.2 | Calculated losses due to Fresnel, lateral misalignments and total loss for all sensor lengths | 61 |
| 4.3 | RI range, sensitivity and R-square values for all sensors | 66 |
| 4.4 | Comparison of sensitivity performance between previous techniques and proposed technique | 66 |
| 4.5 | Measured temperature sensitivity and the R-square value for all sensors | 71 |
| 4.6 | Summary of RI sensitivity, temperature sensitivity and cross-sensitivity of all sensors | 71 |
| 4.7 | Temperature sensitivity of modified structure at different surrounding materials | 76 |
| 4.8 | Comparison of temperature sensitivity in previous study with current work | 77 |
| 4.9 | FSR value determined from the calculation, simulation | 78 |

and experimental work

4.10 ER value from the simulation and experiment works 79

LIST OF FIGURES

| FIGURE NO. | TITLE | PAGE |
|------------|---|------|
| 1.1 | Basic elements in optical fiber sensing system | 2 |
| 1.2 | Classification of fiber optic sensors | 4 |
| 2.1 | Intrinsic FPI sensor with two reflecting components (R_1 and R_2) and (b) extrinsic FPI sensor formed by an external air cavity | 11 |
| 2.2 | Schematic diagram of extrinsic FPI sensor with external packaging | 12 |
| 2.3 | Schematic diagram of Michelson Interferometer | 13 |
| 2.4 | Schematic diagram of MZI | 14 |
| 2.5 | Illustration that defined FSR and ER of an interference spectrum | 16 |
| 2.6 | MZI based on combine tapered-core offset structure | 18 |
| 2.7 | (a) Schematic diagram of two ultra-abrupt tapers RI sensor, (b) top view of removed part using femtosecond laser | 19 |
| 2.8 | (a) Single mode tapered structure used for protein sensing and (b) Thinned fiber taper with high RI sensitivity | 19 |
| 2.9 | Sharp tapered PCF sensor that introduced to improve | 21 |

| | | |
|------|---|----|
| | RI sensitivity of previous sensor based on collapse region of PCF | |
| 2.10 | Half taper collapsed region structure | 21 |
| 2.11 | (a) Peanut shape structure was implement for RI measurement, (b) modified peanut shape structure with additional tapered region | 23 |
| 2.12 | Sensor structure based on (a) SMF-MMF-SMF, (b) SMF-MMF-FBG, (c) SMF-TCF-MMF-SMF, (d) SMF-TCF-MMF-TCF-SMF and (e) SMSMS | 24 |
| 2.13 | Lateral offset RI sensor with a FBG for sensor length (a) 66mm and (b) 7.1 cm | 26 |
| 2.14 | RI sensor based on lateral offset and tapered MZI structure | 27 |
| 2.15 | Large offset structure of RI gas sensor | 28 |
| 2.16 | Propagation of light in SMF-CSF | 34 |
| 3.1 | Flowchart of research methodology | 38 |
| 3.2 | Schematic structure of proposed RI sensor | 40 |
| 3.3 | Adjustment of lead-out CSF section to observe changes of output spectrum before it is spliced at maximum fringe visibility | 42 |
| 3.4 | Sensor structure in BeamPROP software | 44 |
| 3.5 | Graphical user interface of Symbol Table Editor | 44 |
| 3.6 | MOST Optimizer is used to find the optimum offset distance and active variable in MOST optimizer indicated by alphabet Y | 46 |
| 3.7 | Captured SMF-CSF spliced image in automatic fusion splicer | 47 |

| | | |
|------|--|----|
| 3.8 | (a) Schematic diagram of splicing process at the first splice joint and (b) Captured image of spliced fiber at the first offset splice joint in the fusion splicer | 48 |
| 3.9 | Final steps involved in fabrication of sensor | 49 |
| 3.10 | Captured image of sensor structures from microscope | 49 |
| 3.11 | Experimental setup for RI measurements | 51 |
| 3.12 | Image of sensor placed on the plate | 51 |
| 3.13 | Experimental setup for temperature measurement | 52 |
| 4.1 | Simulated spectra of sensor A, B and C at different offset distance in background index of 1.33 | 55 |
| 4.2 | Optimum offset distance for different sensor lengths | 57 |
| 4.3 | Full schematic diagram of sensor structure for three different sample; Sensor A, B and C | 58 |
| 4.4 | Distinguishable fringe visibility of simulated output spectra for sensor C (1.5mm) | 59 |
| 4.5 | Simulated field distribution in background index 1.330 for sensor (a) A, (b) B and (c) C | 60 |
| 4.6 | (a) Transmission spectra and (b) the linear fit of dip wavelength shift for sensor A | 62 |
| 4.7 | (a) Transmission spectra and (b) the linear fit of dip wavelength shift for sensor B | 63 |
| 4.8 | (a) Transmission spectra and (b) the linear fit of dip wavelength shift for sensor C | 64 |
| 4.9 | (a) Measured spectra of sensor A with temperature variations and (b) Linear fitted of wavelength shift of the dip as a function of temperature | 67 |

| | | |
|------|---|----|
| 4.10 | (a) Measured spectra of sensor B with temperature variations and (b) Linear fitted of wavelength shift of the dip as a function of temperature | 68 |
| 4.11 | (a) Measured spectra of sensor C with temperature variations and (b) Linear fitted of wavelength shift of the dip as a function of temperature | 69 |
| 4.12 | Measured output spectra at different oven temperature and its corresponding wavelength dip in ten minutes' interval | 72 |
| 4.13 | Modified structure in different surrounding material (RI liquid, water and air) for improvement of temperature sensitivity | 74 |
| 4.14 | (a) Interference spectra of sensor in air surrounding measured at different temperatures and (b) linear fitted of wavelength shift versus temperature | 75 |
| 4.15 | (a) Interference spectra of sensor in water surrounding measured at different temperatures and (b) linear fitted of wavelength shift versus temperature | 75 |
| 4.16 | (a) Interference spectra of sensor in RI surrounding measured at different temperatures and (b) linear fitted of wavelength shift versus temperature | 76 |
| 4.17 | (a) Simulated spectra in 1.33 background index, (b) Measured output spectra in 1.33 background index | 77 |

LIST OF ABBREVIATIONS

| | | |
|-----|---|-----------------------------------|
| FOS | - | Fiber optic sensor |
| UV | - | Ultraviolet |
| FPI | - | Fabry Perot Interferometer |
| MI | - | Michelson Interferometer |
| MZI | - | Mach Zehnder Interferometer |
| MMF | - | Multimode fiber |
| RI | - | Refractive index |
| PCF | - | Photonic Crystal fiber |
| SMF | - | Single mode fiber |
| OSA | - | Optical spectrum analyzer |
| HCF | - | Hollow core fiber |
| ER | - | Extinction ratio |
| FSR | - | Free spectra ratio |
| TOC | - | Thermo optic coefficient |
| TEC | - | Thermal expansion coefficient |
| TCF | - | Thin core fiber |
| SMS | - | Single mode-multimode-single mode |
| FBG | - | Fiber Bragg Gratings |
| CSF | - | Coreless Silica fiber |
| MMI | - | Multimode interference |
| RIU | - | Refractive index unit |

LIST OF APPENDICES

| APPENDIX | TITLE | PAGE |
|-----------------|-----------------------------|-------------|
| A | Derivation of MZI Equations | 92 |
| B | List of Publication | 94 |

CHAPTER 1

INTRODUCTION

1.1 Introduction

Referring to the American National Standards Institute [1], sensor is a device that provides a usable output in response to changes of specific quantities. The output of sensor can be in electrical signal (conventional sensor) or optical signals (optical sensor). Due to its well-known advantageous such as immunity to electromagnetic interference, small size and cost effective, fiber optic sensor (FOS) becomes more preferable in niche applications where the conventional electrical sensors are impractical. FOS is also capable to operate in harsh environment and at the same time provides comparable performance to the electronic sensors. With better performance and more reliable telecommunication links, the revolution also brings more benefits to FOS industry by “spin-off” the production of optical components in high volume rate. Thus, the growth of FOS technology becomes faster due to dramatically reduce of optical component price [2]. Until now, FOS technology is continuously researched to fulfill the needs of new emerging applications. FOS are being used in medical [3], [4], structural health monitoring of aircraft [5] and building structure [6], oil and gas industry [7] and also in food industry [8].

1.2 Fiber Optic Sensor

Figure 1.1 shows the basic components of an optical fiber sensing system. It consists of a light source, optical fibers and a detector. Light emits from the light source will propagate through the optical fibers. When light passes through the sensor head, external perturbations (i.e. physical parameters) cause changes in optical properties. These physical parameters can be quantified from the changes of optical properties such as intensity (amplitude), frequency, polarization and phase. Wavelength-based sensing technique is one of the promising techniques available, whereby sensor response is measured from the wavelength change of the output spectra. The optical signal that contains sensing information is detected by the optical detector.

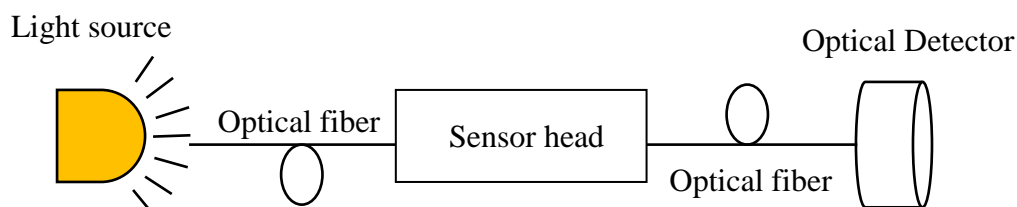


Figure 1.1 Basic elements in optical fiber sensing system

Among the typical FOS types available are the fiber laser [9]–[11], fiber gratings [3], [12] and fiber interferometer [13]–[15]. Fiber grating is a periodical change of refractive index on single mode fiber (SMF) which can be formed by high intensity UV laser scanning with a phase mask. It is considered as the most established and reliable technique in fiber sensor, however it also comes with the high manufacturing cost. Fiber laser is basically a fiber grating that written on active fiber such the erbium-doped fiber. While a fiber laser system is typically more complex than the fiber grating system, it is also provides much better performance and desirable for high end military applications such as hydrophone. Generally, implementation of fiber optic interferometer sensor is much simpler and cost effective compared to fiber gratings and fiber laser. Fiber interferometer has been used to detect various physical parameters such as temperature, refractive

index (RI), curvature, strain, vibration, and displacement. As shown in Figure 1.2, the major interferometer types can be categorized into Fabry Perot Interferometer (FPI) [16]-[17], Michelson Interferometer (MI) [18]–[20], Mach-Zehnder Interferometer (MZI) [21]–[23] and composite interferometer [24].

There several techniques have been developed in order to produce RI sensor based on MZI. Among the available techniques in previous research including the implementation of lateral offset structure [14], [25]–[28], fiber taper method [29], [30] and large core diameter of MMF [31], [32]. In essence, there are two types of lateral offset structure being adopted in previous research. The first type involves offsetting the first fiber core with small lateral offset such that the light can spread into the core and cladding of the sensing fiber. Hence, detection is established from the interaction between the cladding modes with the surrounding perturbation [27], [28]. In contrast, the second type of the techniques requires large offset such that light from the lead in fiber is directly spread into the surrounding (e.g. air and liquid), as well as the cladding of a fiber, which creates two distinct interferometer arms with large RI difference. As a result, higher RI sensitivity can achieve attributed to direct interaction with the surrounding material [14]. Due to its high sensitivity from direct interaction, the sensor may be realized with small sensor size which is very much desired in practical applications. However, it is believed that the existing designs require high fabrication precision which may difficult to implement using basic splicing equipment. This work proposed a new sensor design based on lateral offset of coreless silica fiber to overcome high fabrication tolerance requirement and at the same time retain the advantages of the direct interaction type sensor. Performance comparison between different techniques applied in the RI sensor will be presented in Table (2.1) at the end of Chapter 2 to justify the achievement of the proposed sensor.

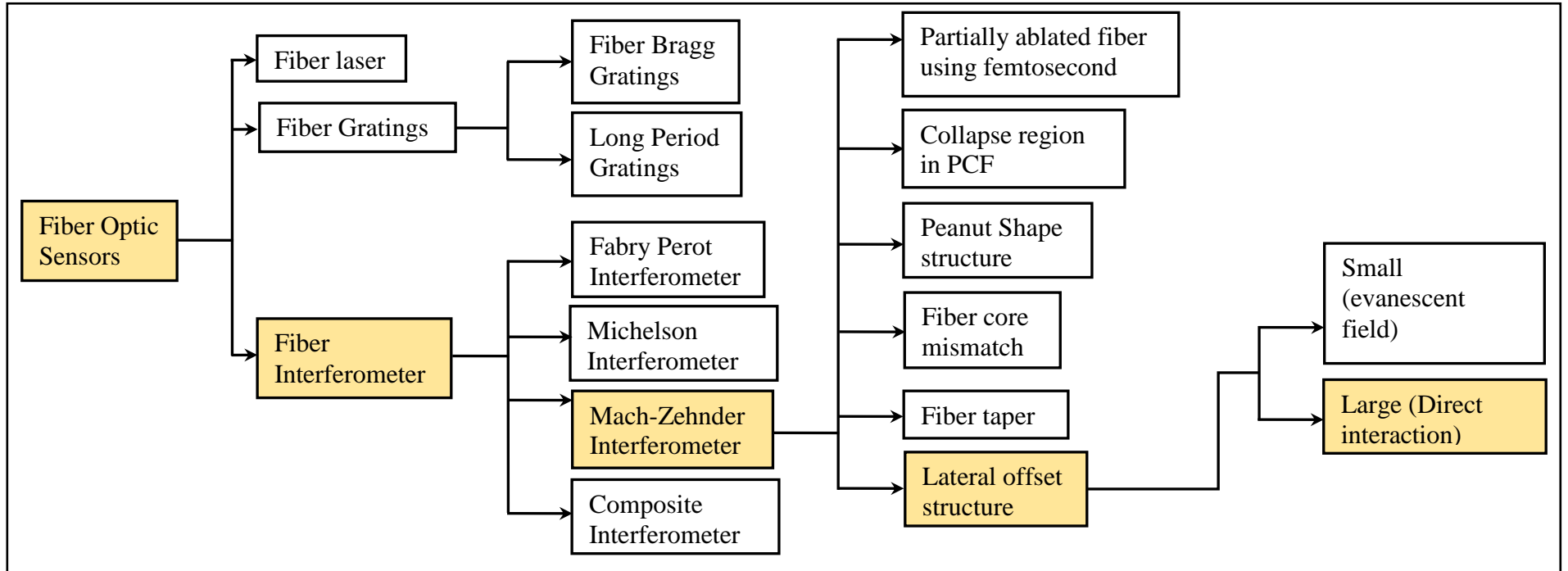


Figure 1.2 Classification of fiber optic sensors

1.3 Problem Statement

There are several techniques employed to realize fiber MZI for RI sensing in the way that light is split into two different optical paths. Sensing performance has been continuously improved with new designs. Basically, the key performance parameters of a sensor are the RI sensitivity, easiness of fabrication process and sensor head size. Tapering [33] and laser ablation [34] techniques may require expensive tapering machine and laser system to perform the fabrication. Meanwhile sensor based on PCF [35]–[37], peanut structure [38] and fiber core mismatched [39], [40] techniques can be fabricated using basic splicing equipment. However, all of these techniques rely on evanescent field interaction of cladding modes with the surrounding which is feasible by long optical path (which translates to sensor head size) in the range of few centimeters. Their sensitivity can be improved by fiber tapering [35], [41] to enhance cladding mode leakage to surrounding. On the other hand, lateral offset technique can be further categorized into small offset and large offset techniques. Small offset technique [26], [27], [42] is basically identical to the PCF collapsed region, peanut structure and fiber core mismatched techniques in terms of its sensing mechanism which is based on evanescent field interaction. Thus, it has the similar disadvantages as have been discussed. Several research works have demonstrated that the large lateral offset structure for RI measurement is capable to improve the sensitivity performance up to thousands nm/RIU if compared with a few micrometer offset distance structure. Previous research [14] involved with the use of single mode fiber as the sensing element in the lateral offset structure which is subjected to high precision requirement as the core diameter of the SMF is typically around 9 μm . Thus, allowable offset distance is only a few micrometers from core center in order to ensure the functionality of sensor. This suggests that slight misalignment in the range of micrometers could lead to unworkable sensor. In this work, coreless silica fiber with diameter of 125 μm is proposed to reduce stringent alignment requirement during fabrication and at the same time retain the high sensitivity of large offset structure.

1.4 Objectives of Research

From the problem statement in the previous section, the objectives of this research can be stated as follows:

- 1) To develop a compact size refractive index sensor based on large lateral-offset structure of coreless silica fiber.
- 2) To characterize the sensor response towards refractive index changes through experimental work.
- 3) To test the applicability of the sensor structure in high sensitivity temperature sensing.

1.5 Scope of Study

In order to provide a clear research overview, the scope of study is divided into two main parts which are design and simulation, and experimental work.

1.5.1 Design and simulation

The use of large offset structure in RI measurement is motivated from the development of the same structure for measurement of RI gas in previous study [14]. The reported study which attained great sensitivity performance was demonstrated using conventional SMF. Considering high alignment accuracy requirement using the SMF in the study, we propose a novel structure based on CSF to improve the suggested fabrication problem as previously discussed in section 1.3. In simulation works, the characteristics of proposed sensor structures with three different lengths are investigated. The effects of changing the offset distance at both offset splicing joints are observed while the optimum offset distance for a particular sensor length is chosen based on highest fringe visibility of simulated output spectra. Then, using the

optimized offset distance that determined from previous step, the simulation is further executed to generate field distribution along the fiber structures.

1.5.2 Experimental works

Experimental works involved fabrication, experimental setup and sensor testing. All of these works are carried out using in-house facility. Experimental setup to measure RI and temperature response of the sensor is prepared for both RI and temperature measurement. RI solutions with range 1.300 to 1.350 are used for RI measurement. Meanwhile, the sensors were tested in temperature variations between 30 °C to 100 °C in order to investigate the susceptibility for temperature measurement. Further investigation to enhance the temperature sensitivity was also investigated and tested in lower temperature range between 26 °C to 30 °C. Labview software is used for real-time data acquisition. The recorded data from RI and temperature measurement are analysed offline by using Matlab software.

1.6 Significance of Study

Fiber optic RI sensors are widely used in industrial application such as biomedical, manufacturing and health monitoring system due to its well-known advantages over the conventional electrical sensor such as immune to electromagnetic interference, compact size and ruggedness performance in harsh surrounding conditions. Hence, it is crucial to provide better approach in order to produce the sensors in bulk quantity specifically for the industrial application. Previously, RI sensor based-MZI structure have been widely researched by develop various fabrication techniques. It is expected that MZI sensor based on large offset structure possess high potential in RI measurements, considering the direct interaction of fiber cladding with the measurands. In this study, emphasis is given on the sensitivity performance of large offset structure, and compact sensor design as it is more

preferable many of practical applications. Through implementation of systematic design process and fabrication procedures, high RI sensitivity has been achieved. The proposed structure is highly flexible as it can be utilized for detection of other parameters such as temperature, magnetic field, gas and relative humidity by simple setup adjustment. This is possible as long as the sensing mechanism relies on the change of RI at the second optical path. In this work, feasibility of the structure for high sensitivity temperature measurement is also demonstrated by filling the gap area with high thermo-optic RI liquid.

1.7 Thesis Overview

Chapter 1 presents the basic operations of fiber optic sensor. Starting from the basic principle of fiber optic sensor, FOS is further described. Classification of fiber interferometers are then made based on the existing techniques that have been achieved in previous studies such as collapsed region of PCF, fiber core mismatch, lateral offset structure and etcetera. Then, the formulated research problems are briefly explained which mainly concerned on the high tolerance requirement for fabrication process and low sensitivity performance of lateral offset structure using conventional SMF. The objectives of research and the scope of study are also presented.

In Chapter 2, large growing body of literature review consist of three types of fiber interferometers including FPI, MI and MZI and their recent performance are further elaborated. All the related equations of MZI principle are presented to understand how the proposed structure response to RI and temperature changes. Discussion are also broadly covers the existing methods that have been used to develop the MZI sensor in previous study. The selection of CSF and recent development of CSF in application of fiber optic sensor has been discussed in detail at the end of the chapter.

While in Chapter 3, details on design specification and working principles of the sensor structure are presented. The steps involved to investigate the characteristics and sensitivity performance of the sensor including feasibility test, simulation work using BeamPROP software, fabrication procedure and the experimental works have been included.

Simulation and experimental findings are reported in Chapter 4. In general, there are two important result that have been extracted from the simulation results which are the optimized sensor design and distributed light along the fiber structures. The sensitivity performance of proposed sensor has been characterized based on the response in RI measurement. The response of sensor towards temperature variations and the long term stability characteristic of the sensor are also examined. The application of proposed structure for low temperature sensing is further investigated with a slight modification onto the sensor head.

Finally, Chapter 5 concludes all the outcomes of the research works. All suggested works as expansion of current topic the is also provided.

REFERENCES

- [1] N. R. Council, *Expanding the Vision of Sensor Materials*. 1995.
- [2] F. T. S. Yu, *Fiber Optic Sensors*. 2002.
- [3] Y. Rao, D. J. Webb, D. A. Jackson, L. Zhang, and I. Bennion, “In-Fiber Bragg-Grating Temperature Sensor System for Medical Applications,” vol. 15, no. 5, pp. 779–785, 1997.
- [4] M. I. Zibaii, H. Latifi, and F. Karami, “In vivo brain temperature measurements based on fiber optic Bragg grating,” no. 1, pp. 3–6, 2017.
- [5] R. Di Sante, “Fibre Optic Sensors for Structural Health Monitoring of Aircraft Composite Structures: Recent Advances and Applications,” pp. 18666–18713, 2015.
- [6] Z. Yazdizadeh, H. Marzouk, and M. Ali, “Monitoring of concrete shrinkage and creep using Fiber Bragg Grating sensors,” *Constr. Build. Mater.*, vol. 137, pp. 505–512, 2017.
- [7] S. Zhi and L. Sheng, “Optical Fiber Technology Performance enhancement of BOTDR fiber optic sensor for oil and gas pipeline monitoring,” *Opt. Fiber Technol.*, vol. 16, no. 2, pp. 100–109, 2010.
- [8] N. Bidin, N. H. Zainuddin, S. Islam, M. Abdullah, F. M. Marsin, and M. Yasin, “Sugar Detection in Adulterated Honey via Fiber Optic Displacement Sensor for Food,” vol. 16, no. 2, pp. 299–305, 2016.
- [9] A. I. Azmi *et al.*, “Fiber Laser Based Hydrophone Systems,” *Photonic Sensors*, vol. 1, no. 3, pp. 210–221, 2011.
- [10] X. Hao, Z. Tong, W. Zhang, and Y. Cao, “A fiber laser temperature sensor based on SMF core-offset structure,” *Opt. Commun.*, vol. 335, pp. 78–81, 2015.
- [11] Q. Meng, X. Dong, K. Ni, and Z. Chen, “Optical Fiber Laser Sensor for Refractive Index Measurement,” no. 2010, pp. 1–4, 2013.
- [12] H. Tsuda and K. Urabe, “Characterization of long-period grating refractive index sensors and their applications,” *Sensors (Switzerland)*, vol. 9, no. 6, pp. 4559–4571, 2009.
- [13] M. Sun, Y. Jin, and X. Dong, “All-Fiber Mach – Zehnder Interferometer for Liquid Level Measurement,” vol. 15, no. 7, pp. 3984–3988, 2015.

- [14] D. W. Duan, Y. J. Rao, L. C. Xu, T. Zhu, D. Wu, and J. Yao, "In-fiber Mach-Zehnder interferometer formed by large lateral offset fusion splicing for gases refractive index measurement with high sensitivity," *Sensors Actuators, B Chem.*, vol. 160, no. 1, pp. 1198–1202, 2011.
- [15] N. F. Baharin, A. I. Azmi, A. S. Abdullah, and M. Y. Mohd Noor, "Refractive index sensor based on lateral-offset of coreless silica interferometer," *Opt. Laser Technol.*, vol. 99, pp. 396–401, 2018.
- [16] T. Wei, Y. Han, H.-L. Tsai, and H. Xiao, "Miniaturized fiber inline Fabry-Perot interferometer fabricated with a femtosecond laser.," *Opt. Lett.*, vol. 33, no. 6, pp. 536–538, 2008.
- [17] D. Wu, Y. Huang, J. Y. Fu, and G. Y. Wang, "Fiber Fabry-Perot tip sensor based on multimode photonic crystal fiber," *Opt. Commun.*, vol. 338, pp. 288–291, 2015.
- [18] A. Zhou *et al.*, "Asymmetrical Twin-Core Fiber Based Michelson Interferometer for Refractive Index Sensing," vol. 29, no. 19, pp. 2985–2991, 2011.
- [19] Z. Li *et al.*, "Temperature-insensitive refractive index sensor based on in-fiber Michelson interferometer," *Sensors Actuators B. Chem.*, vol. 199, pp. 31–35, 2014.
- [20] Z. Liang, C. Zhao, and B. Wu, "Optical Fiber Refractive Index Sensor based on Peanut Flat-end Reflection Structure Corresponding author : Chunliu Zhao E-mail : zhchunliu@hotmail.com," pp. 15–17, 2016.
- [21] H. Y. Choi, M. J. Kim, and B. H. Lee, "All-fiber Mach-Zehnder type interferometers formed in photonic crystal fiber.," *Opt. Express*, vol. 15, no. 9, pp. 5711–5720, 2007.
- [22] D. Yuan, Y. Dong, Y. Liu, and T. Li, "Mach-Zehnder Interferometer Biochemical Sensor Based on Silicon-on-Insulator Rib Waveguide with Large Cross Section," pp. 21500–21517, 2015.
- [23] Y. Zhao, F. Xia, H. Hu, and M. Chen, "A novel photonic crystal fiber Mach – Zehnder interferometer for enhancing refractive index measurement sensitivity," *Opt. Commun.*, vol. 402, no. June, pp. 368–374, 2017.
- [24] Z. Tong, J. Su, Y. Cao, and W. Zhang, "Simultaneous Measurement Based on Composite Interference Structure," vol. 26, no. 13, pp. 1310–1313, 2014.
- [25] D. Duan, Y. Rao, and T. Zhu, "High sensitivity gas refractometer based on all-

- fiber open-cavity Fabry – Perot interferometer formed by large lateral offset splicing,” vol. 29, no. 5, pp. 912–915, 2012.
- [26] Y. Zhao, X. Li, and L. Cai, “A highly sensitive Mach–Zehnder interferometric refractive index sensor based on core-offset single mode fiber,” *Sensors Actuators A Phys.*, vol. 223, pp. 119–124, 2015.
- [27] Q. Yao *et al.*, “Simultaneous measurement of refractive index and temperature based on a core-offset Mach-Zehnder interferometer combined with a fiber Bragg grating,” *Sensors Actuators, A Phys.*, vol. 209, pp. 73–77, 2014.
- [28] Z. Tian, G. S. Member, S. S. Yam, and H. Look, “Single-Mode Fiber Refractive Index Sensor Based on Core-Offset Attenuators,” vol. 20, no. 16, pp. 1387–1389, 2008.
- [29] Z. Tian *et al.*, “Refractive Index Sensing With Mach – Zehnder Interferometer Based on Concatenating Two Single-Mode Fiber Tapers,” vol. 20, no. 8, pp. 626–628, 2008.
- [30] B. Li, “Ultra-Abrupt Tapered Fiber Mach-Zehnder Interferometer Sensors,” pp. 5729–5739, 2011.
- [31] Y. Ma *et al.*, “Mach-Zehnder interferometer based on a sandwich fiber structure for refractive index measurement,” *IEEE Sens. J.*, vol. 12, no. 6, pp. 2081–2085, 2012.
- [32] Yong Zhao, Lu Cai, and Xue-Gang Li, “High Sensitive Modal Interferometer for Temperature and Refractive Index Measurement,” *IEEE Photonics Technol. Lett.*, vol. 27, no. 12, pp. 1341–1344, 2015.
- [33] T. K. Yadav, R. Narayanaswamy, M. H. A. Bakar, Y. M. Kamil, and M. A. Mahdi, “Single mode tapered fiber-optic interferometer based refractive index sensor and its application to protein sensing,” vol. 22, no. 19, pp. 22802–22807, 2014.
- [34] Y. Wang, M. Yang, D. N. Wang, S. Liu, and P. Lu, “Fiber in-line Mach Zehnder interferometer fabricated by femtosecond laser micromachining for refractive index measurement with high sensitivity,” vol. 27, no. 3, pp. 370–374, 2010.
- [35] C. Li, S. Qiu, Y. Chen, F. Xu, and Y. Lu, “Ultra-Sensitive Refractive Index Sensor With Slightly Tapered Photonic Crystal Fiber,” *IEEE Photonics Technol. Lett.*, vol. 24, no. 19, pp. 1771–1774, 2012.
- [36] H. Gong, C. Chan, F. Zhang, C. Wong, and X. Dong, “Miniature

- refractometer based on modal interference in a hollow-core photonic crystal fiber with collapsed splicing,” *J. Biomed. Opt.*, vol. 16, no. January, pp. 2–5, 2011.
- [37] N. F. Baharin *et al.*, “Hollow-Core Photonic Crystal Fiber Refractive Index,” *ARPJ. Eng. Appl. Sci.*, vol. 11, no. 9, pp. 5702–5706, 2016.
- [38] R. Huang, K. Ni, X. Wu, and Q. Ma, “Refractometer based on Mach – Zehnder interferometer with peanut- shape structure,” *Opt. Commun.*, vol. 353, pp. 27–29, 2015.
- [39] J. Huang, X. Lan, A. Kaur, H. Wang, L. Yuan, and H. Xiao, “Temperature compensated refractometer based on a cascaded SMS/LPFG fiber structure,” *Sensors Actuators, B Chem.*, vol. 198, pp. 384–387, 2014.
- [40] Q. Wu, Y. Semenova, P. Wang, and G. Farrell, “High Sensitivity SMS Fiber Structure Based Refractometer – Analysis and Experiment,” *Opt. Express*, 2011.
- [41] R. Huang, K. Ni, Q. Ma, and X. Wu, “Refractometer based on a tapered Mach – Zehnder interferometer with Peanut-Shape structure,” *Opt. Lasers Eng.*, vol. 83, pp. 80–82, 2016.
- [42] X. Yu, X. Chen, D. Bu, J. Zhang, and S. Liu, “In-fiber modal interferometer for simultaneous measurement of refractive index and temperature,” *IEEE Photonics Technol. Lett.*, vol. 28, no. 2, pp. 1–1, 2016.
- [43] F. G. Smith, *Optics and Photonics : An Introduction Second Edition*, vol. 69. 2007.
- [44] T. Zhao, “Fiber Optic Fabry – Perot strain sensor based on graded-index multimode fiber,” vol. 9, no. 5, pp. 1–4, 2011.
- [45] Y. Zhang, X. Chen, Y. Wang, K. L. Cooper, and A. Wang, “Microgap multicavity Fabry-Pérot biosensor,” *J. Light. Technol.*, vol. 25, no. 7, pp. 1797–1804, 2007.
- [46] V. R. Machavaram, R. A. Badcock, and G. F. Fernando, “Fabrication of intrinsic fibre Fabry-Perot sensors in silica fibres using hydrofluoric acid etching,” *Sensors Actuators, A Phys.*, vol. 138, no. 1, pp. 248–260, 2007.
- [47] Z. Ran, Y. Rao, J. Zhang, Z. Liu, and B. Xu, “A miniature fiber-optic refractive-index sensor based on laser-machined Fabry-Perot interferometer tip,” *J. Light. Technol.*, vol. 27, no. 23, pp. 5426–5429, 2009.
- [48] Y.-J. Rao, M. Deng, D.-W. Duan, X.-C. Yang, T. Zhu, and G.-H. Cheng,

- “Micro Fabry-Perot interferometers in silica fibers machined by femtosecond laser,” *Opt. Express*, vol. 15, no. 21, pp. 14123–14128, 2007.
- [49] Z. L. Ran, Y. J. Rao, W. J. Liu, X. Liao, and K. S. Chiang, “Laser-micromachined Fabry-Perot optical fiber tip sensor for high-resolution temperature-independent measurement of refractive index,” *Opt. Express*, vol. 16, no. 3, p. 2252, 2008.
- [50] P. P. Shum, P. Zhang, M. Tang, F. Gao, B. Zhu, and Z. Zhao, “Simplified Hollow-Core Fiber-Based Fabry – Perot Interferometer With Modified Vernier Effect for Highly Sensitive High-Temperature Measurement Simplified Hollow-Core Fiber-Based Fabry – Perot Interferometer With Modified Vernier Effect for Highly Sensitive,” vol. 7, no. 1, 2015.
- [51] Y. Lu, J. Tian, Y. Lu, Q. Zhang, and M. Han, “Microfluidic refractive index sensor based on an all-silica in-line Fabry – Perot interferometer fabricated with microstructured fibers,” no. March 2013, 2015.
- [52] R. Gao, Y. Jiang, W. Ding, Z. Wang, and D. Liu, “Filmed extrinsic Fabry – Perot interferometric sensors for the measurement of arbitrary refractive index of liquid,” vol. 177, pp. 924–928, 2013.
- [53] Y. Rao, M. Deng, D. Duan, and T. Zhu, “In-line fiber Fabry-Perot refractive-index tip sensor based on endlessly photonic crystal fiber,” vol. 148, pp. 33–38, 2008.
- [54] J. Zhang, H. Sun, Q. R. Â. Ö, Y. M. Ì, and L. Liang, “High-temperature sensor using a Fabry-Perot interferometer based on solid-core photonic crystal fiber,” vol. 10, no. 7, pp. 2–4, 2012.
- [55] M. Deng, C. Tang, T. Zhu, Y. Rao, L. Xu, and M. Han, “Refractive index measurement using photonic crystal fiber-based Fabry – Perot interferometer,” vol. 49, no. 9, pp. 1593–1598, 2010.
- [56] J. Zhou *et al.*, “Intensity modulated refractive index sensor based on optical fiber Michelson interferometer,” *Sensors Actuators, B Chem.*, vol. 208, pp. 315–319, 2015.
- [57] D. W. Kim, Y. Zhang, K. L. Cooper, and A. Wang, “In-fiber reflection mode interferometer based on a long-period grating for external refractive-index measurement,” *Appl. Opt.*, vol. 44, no. 26, p. 5368, 2005.
- [58] G. Yin, S. Lou, and H. Zou, “Refractive index sensor with asymmetrical fiber Mach – Zehnder interferometer based on concatenating single-mode abrupt

- taper and core-offset section,” vol. 45, no. 3, pp. 294–300, 2013.
- [59] P. Lu, L. Men, K. Sooley, and Q. Chen, “Tapered fiber Mach – Zehnder interferometer for simultaneous measurement of refractive index and temperature,” pp. 1–3, 2009.
- [60] J. Yang *et al.*, “High sensitivity of taper-based Mach – Zehnder interferometer embedded in a thinned optical fiber for refractive index sensing,” vol. 50, no. 28, pp. 5503–5507, 2011.
- [61] Y. Miao *et al.*, “Low-Temperature Cross-Sensitivity Refractive Index Sensor based on Single-Mode Fiber with Periodically Modulated Taper,” *IEEE Sens. J.*, vol. 16, no. 8, pp. 2442–2446, 2016.
- [62] F. Ahmed *et al.*, “Miniaturized Tapered Photonic Crystal Fiber Mach – Zehnder Interferometer for Enhanced Refractive Index Sensing,” *IEEE Sens. J.*, vol. 16, no. 24, pp. 8761–8766, 2016.
- [63] R. Huang, K. Ni, X. Wu, and Q. Ma, “Refractometer based on Mach–Zehnder interferometer with peanut-shape structure,” *Opt. Commun.*, vol. 353, pp. 27–29, 2015.
- [64] Q. Wu, Y. Semenova, P. Wang, and G. Farrell, “High sensitivity SMS fiber structure based refractometer – analysis and experiment,” *Opt. Express*, vol. 19, no. 9, p. 7937, 2011.
- [65] Y. Zhao, L. Cai, X. G. Li, and F. C. Meng, “Liquid concentration measurement based on SMS fiber sensor with temperature compensation using an FBG,” *Sensors Actuators, B Chem.*, vol. 196, pp. 518–524, 2014.
- [66] Q. Rong and R. Wang, “Temperature-calibrated fiber-optic refractometer based on a compact FBG-SMS structure,” vol. 10, no. 3, pp. 3–5, 2012.
- [67] M. Shao, X. Qiao, H. Fu, H. Li, Z. Jia, and H. Zhou, “Refractive Index Sensing of SMS Fiber Structure Based Mach-Zehnder Interferometer,” vol. 26, no. 5, pp. 437–439, 2014.
- [68] H. Fu *et al.*, “TCF-MMF-TCF fiber structure based interferometer for refractive index sensing,” *Opt. Lasers Eng.*, vol. 69, pp. 58–61, 2015.
- [69] J. Shi, S. Xiao, and M. Bi, “Sensitivity-enhanced refractive index sensor by using tapered thin-core fiber based inline Mach-Zehnder interferometer,” vol. 8311, no. 1, pp. 1–6, 2011.
- [70] P. S. J. R. J. C. Knight, T. A. Birks, “Properties of Photonic Crystal Fiber and the Effective Index Mode,” *Opt. Soc. Am.*, vol. 15, no. 3, pp. 748–752, 1998.

- [71] J. Kumar, R. Mahakud, U. Kumbhkar, O. Prakash, S. K. Dixit, and S. V. Nakhe, "Optik Analysis of experimental results on the adulteration measurement by an etched fiber Bragg grating sensor," vol. 126, pp. 5698–5702, 2015.
- [72] Y. Zhao, X. Li, and L. Cai, "Mach–Zehnder interferometer formed by a large core-offset splicing fiber for temperature and displacement measurement," *Opt. Commun.*, vol. 356, pp. 54–58, 2015.
- [73] Thorlabs.com, "Datasheet Coreless silica fibre," 2017, pp. 9–10.
- [74] L. Ma, Z. Kang, Y. Qi, and S. Jian, "Fiber-optic temperature sensor based on a thinner no-core fiber," *Opt. - Int. J. Light Electron Opt.*, vol. 126, no. 9–10, pp. 1044–1046, 2015.
- [75] W.-F. L. Lung-Shiang Huang, Guei-Ru Lin, Ming-Yue Fu³, Hao-Jan Sheng, Hai-Tao Sun, "A Refractive-index Fiber Sensor by Using No-Core Fiber," no. 100, pp. 100–102, 2013.
- [76] G. Lin, M. Fu, C. Lee, and W. Liu, "Dual-parameter sensor based on a no-core fiber and fiber Bragg grating," 2015.
- [77] X. Zhou, K. Chen, X. Mao, and Q. Yu, "A reflective fiber-optic refractive index sensor based on multimode interference in a coreless silica fiber," *Opt. Commun.*, vol. 340, pp. 50–55, 2015.
- [78] Y. Chen *et al.*, "A Hybrid Multimode Interference Structure- Based Refractive Index and Temperature Fiber Sensor A hybrid multimode interference structure based refractive index and temperature fiber sensor," no. January 2016, 2015.
- [79] T. Erdogan, "Cladding-mode resonances in short- and long- period fiber grating filters," vol. 14, no. 8, pp. 1760–1773, 1997.
- [80] J. Senior, *Optical Fiber Communications*, Third. Prentice Hall, 2009.
- [81] J. Fan, J. Zhang, P. Lu, M. Tian, J. Xu, and D. Liu, "A single-mode fiber sensor based on core-offset inter-modal interferometer," *Opt. Commun.*, vol. 320, pp. 33–37, 2014.
- [82] L. Li, L. Xia, Y. Wuang, Y. Ran, C. Yang, and D. Liu, "Novel NCF-FBG Interferometer for Simultaneous Measurement of Refractive Index and Temperature," vol. 24, no. 24, pp. 2268–2271, 2012.
- [83] X. Shu, L. Zhang, and I. Bennion, "Sensitivity Characteristics of Long-Period Fiber Gratings," vol. 20, no. 2, pp. 255–266, 2002.

- [84] J. Grochowski, M. My, P. Mikulic, and W. J. Bock, "Temperature Cross-Sensitivity for Highly Refractive Index Sensitive Nanocoated Long-Period Gratings," vol. 124, no. 3, pp. 421–424, 2013.
- [85] D. Wu, T. Zhu, K. S. Chiang, and M. Deng, "All single-mode fiber mach-zehnder interferometer based on two peanut-shape structures," *J. Light. Technol.*, vol. 30, no. 5, pp. 805–810, 2012.
- [86] N. Zazwani R., R. K. Raja Ibrahim, S. M. A. Musa, S. Raheleh Hosseinian, A. I. Azmi, and N. Ahmad, "Reactor temperature profiles of non-thermal plasma reactor using fiber Bragg grating sensor," *Sensors Actuators, A Phys.*, vol. 244, pp. 206–212, 2016.
- [87] Y. Zhang, L. Xue, T. Wang, L. Yang, B. Zhu, and Q. Zhang, "High performance temperature sensing of single mode-multimode-single mode fiber with thermo-optic polymer as cladding of multimode fiber segment," *IEEE Sens. J.*, vol. 14, no. 4, pp. 1143–1147, 2014.
- [88] M. Fuentes-Fuentes, D. May-Arriolja, J. Guzman-Sepulveda, M. Torres-Cisneros, and J. Sánchez-Mondragón, "Highly Sensitive Liquid Core Temperature Sensor Based on Multimode Interference Effects," *Sensors*, vol. 15, no. 10, pp. 26929–26939, 2015.
- [89] B. Xu, J. Li, Y. Li, J. Xie, and X. Dong, "Ultrasensitive temperature sensor based on refractive index liquid-sealed thin-core fiber modal interferometers," *IEEE Sens. J.*, vol. 14, no. 4, pp. 1179–1184, 2014.

APPENDIX B

LIST OF PUBLICATIONS

1. N. F. Baharin, A. I. Azmi, A. S. Abdullah and M. Y. M. Noor. Refractive Index Sensor based on Lateral-Offset of Coreless Silica Interferometer. *Journal of Optics and Laser Technology*, vol. 99, pp. 396-401, 2018.
2. N. F. Baharin, N. Sidek, S. M. A. Musa, A. I. Azmi, A. S. Abdullah and M. E. M. Roslan. Hollow Core Photonic Crystal Fiber Refractive Index Sensor based on Modal Interference. *ARPJ Journal of Engineering and Applied Sciences*, vol. 11, no. 9, pp. 5702-5706, 2016.
3. N. F. Baharin, S. M. A. Musa, N. Sidek, A. I. Azmi, A. S. Abdullah, and M. Y. M. Noor. In-Fiber Interferometer based on Lateral-Offset Coreless Silica Fiber for Temperature and Refractive Index Sensing. *Proceeding of LCRG Colloquium 2017, UTM*, First Edition, pp. 47-52, 2018.
4. S. M. A. Musa, N. F. Baharin, A. I. Azmi, R. K. R. Ibrahim, A. S. Abdullah, M. Y. M. Noor and H. Qi. Double-Clad Fiber Michelson Interferometer for Measurement of Temperature and Refractive Index. *Microwave and Optical Technology Letters*, vol. 60, pp. 822-827, 2018.
5. N. F. Baharin, S. M. A. Musa, A. I. Azmi, M. A. A. Razak, A. S. Abdullah, M. R. Salim, and M. Y. M. Noor. Compact and High Sensitivity Low-Temperature Sensor based on Coreless Silica Fiber Mach-Zehnder Interferometer. *Microwave and Optical Technology Letters (accepted for publication)*.